Composites Part B **??** (2016) ?–?

Doi: 10.1016/j.compositesb.2015.09.003

Towards optimisation of load-time conditions for producing viscoelastically prestressed polymeric matrix composites

Bing Wang, Kevin S. Fancey*

School of Engineering, University of Hull, Hull HU6 7RX, United Kingdom

Abstract

A viscoelastically prestressed polymeric matrix composite (VPPMC) is produced by applying a tensile creep load to polymeric fibres, the load being released before the fibres are moulded into a polymeric matrix. The viscoelastically recovering fibres induce compressive stresses within the matrix, which can improve mechanical properties by up to 50%. This study investigates the feasibility of reducing the creep loading period for VPPMC production. By using nylon 6,6 fibres, we have demonstrated that the previously adopted viscoelastic creep strain, requiring 330 MPa for 24 h, can be achieved over a shorter duration, t_n, using increased creep stress. Thus t_n was 92 min at 460 MPa and 37 min at 590 MPa. Subject to avoiding fibre damage however, it may be possible to reduce t_n further. From the three creep settings, elapsed recovery strain values were similar, as were the Charpy impact test data from corresponding VPPMC samples; i.e. there were no significant differences in impact energy absorption, these being ~56% greater than their control (unstresssed) counterparts.

Keywords: A. Fibres; A. Polymer-matrix composites (PMCs); B. Impact behaviour; D. Mechanical testing; Viscoelasticity.

*Tel: +44-1482-465071; fax: +44-1482-466664.
E-mail address: k.s.fancey@hull.ac.uk

1. Introduction

Previous publications have demonstrated that viscoelastically prestressed polymeric matrix composites (VPPMCs) provide improved mechanical performance relative to counterparts without the prestress. These improvements are most evident for Charpy impact toughness [1-8] and flexural moduli [8-10], in which increases of typically 30-50% have been obtained; also tensile tests have demonstrated modest increases in strength (≥15%) [11]. The VPPMC production process involves two stages: (i) polymeric fibres are stretched under a constant load for a period of time so that they undergo viscoelastic creep; (ii) the fibres are released from the load and

subsequently moulded into a resin matrix (e.g. polyester or epoxy). The previously strained fibres continue to attempt viscoelastic recovery after the matrix has solidified, and this produces compressive stresses in the matrix, which are counterbalanced by residual tension within the fibres. It has been suggested that four mechanisms, resulting from prestress effects, may contribute towards the observed improvements in mechanical properties [5]; i.e. (i) matrix compression impedes crack propagation from external tensile forces; (ii) matrix compression attenuates dynamic overstress effects, reducing probability of fibre fracture outside the immediate area of impact; (iii) residual fibre tension causes the fibres to respond more collectively and thus more effectively to external loads; (iv) residual shear stresses at the fibre–matrix interface regions promote (energy absorbing) debonding over transverse fracture.

A more conventional approach to producing prestressed PMCs is to exploit elastic recovery. Here, fibres (e.g. glass or carbon) are stretched elastically within a mould whilst the surrounding resin matrix solidifies. The resulting elastically prestressed PMCs (EPPMCs) can provide similar mechanical property improvements to those offered by the VPPMC approach, in the form of laminates [12-14] and unidirectional fibre-reinforced composites [15-19]. VPPMC methodology requires the use of polymeric fibres with appropriate viscoelastic properties and most of the research to date has involved nylon 6,6 fibres [1-6,9,11]. Clearly, these fibres are, in terms of strength and stiffness, mechanically inferior to the fibres that can be used for EPPMCs, although performance enhancement has been recently demonstrated with nylon 6,6 fibres (for prestress) commingled with Kevlar fibres [8]. Moreover, VPPMCs using viscoelastically generated prestress from other reinforcements have been successfully demonstrated, i.e. UHMWPE fibres [7,10] and bamboo [20].

Since the fibre stretching and moulding operations are de-coupled, the two-stage approach used in VPPMC production offers great flexibility. A creep load can be applied to a fibre tow with relatively simple equipment. Also, following release of the load, the fibres can be chopped to any length and placed in any orientation within any mould geometry that can be filled with a matrix resin. To date however, all VPPMC-based studies within our laboratory have utilised a creep loading period of 24 h [1-11]. Although this is a convenient period for research purposes, such a lengthy duration would be less practical for VPPMC production in a commercial environment. The purpose of this paper is to consider the first steps towards process optimisation by significantly reducing the creep loading period for VPPMC production. As nylon 6,6 is the most established fibre reinforcement for VPPMCs, this will be the material under investigation.

2. Background

Fig. 1 shows schematically, the strain-time characteristics of a polymeric creep-recovery cycle, with time-dependent components represented by functions based on the Weibull or Kohlrausch-Williams-Watts function [21]. For creep, $\varepsilon_{ctot}(t)$ is the total strain at time t, under an applied constant stress:

$$\varepsilon_{ctot}(t) = \varepsilon_i + \varepsilon_c \left[1 - \exp\left(-\left(\frac{t}{\eta_c} \right)^{\beta_c} \right) \right] \quad (1)$$

Here, ε_i is the instantaneous strain from initial application of the stress and the ε_c function is the time dependent creep strain where η_c is the characteristic life and β_c is the shape parameter. Following removal of the creep stress and the instantaneous recovery ε_e, the remaining recovery strain, $\varepsilon_{rvis}(t)$ is:

$$\varepsilon_{rvis}(t) = \varepsilon_r\left[\exp\left(-\left(\frac{t}{\eta_r}\right)^{\beta_r}\right)\right] + \varepsilon_f \qquad (2)$$

The ε_r function is the time dependent recovery strain with η_r and β_r being the Weibull parameters analogous to Eq. (1). The (non-recoverable) strain from viscous flow is represented by ε_f.

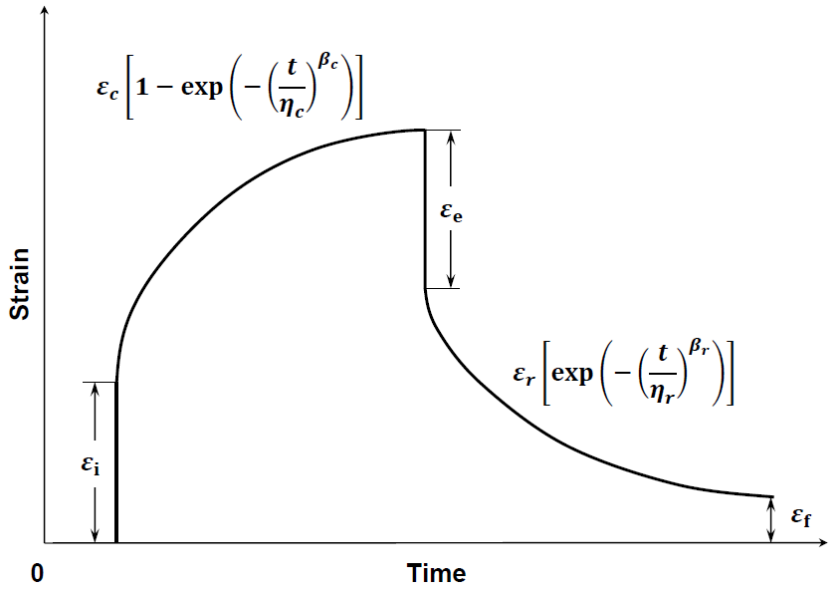

Fig. 1. Schematic tensile creep-recovery strain cycle for a polymeric material.

Clearly, in order to reduce the creep time applied to polymeric fibres for VPPMC production, the applied stress must be increased from the 'standard' 24 h creep stress of ~340 MPa [4-9,11] applied to nylon 6,6 fibres. Using published creep data [22], nylon 6,6 fibre has shown approximately linear viscoelastic properties up to ~50 MPa creep stress over a period exceeding 1000 h but there is increasing deviation from linear viscoelasticity below 100 h [21]. Thus attempting to predict the required creep stress to achieve similar results in a much shorter time than the 24 h creep cycle may be unreliable. Other factors to consider are whether a much higher creep stress (i) increases the risk of failure from fibre fracture during the creep cycle and (ii) causes unwanted changes to the fibre properties. In terms of (ii), the standard 24 h creep stress has been demonstrated to show no adverse effects on the fibres, such as surface damage or changes in short-term tensile test parameters [11].

By considering the above points, an empirical approach is adopted and Fig. 2 illustrates the basic principle. Eq. (1) is used to fit a curve to strain data from the standard run at 24 h, so that after instantaneous strain ε_{i1}, the time-dependent strain value, $\varepsilon_c(24)_{std}$, can be found. Subsequent runs, performed at stress values, σ_n, higher than the standard run, will also provide from Eq. (1), strain values $\varepsilon_c(t_n)$ equal to

$\varepsilon_c(24)_{std}$, where $t_n < 24$ h. Again, $\varepsilon_c(t_n)$ excludes the corresponding instantaneous strain, ε_{i2}. Therefore, a value for t_n which approaches the shortest practical creep time, t_{min}, can be determined, consistent with other factors (no fibre damage) outlined above.
The next step is to compare measurements of recovery strain as a function of time from a run subjected to creep up to t_n, with those obtained from a standard creep run. It may be expected that fitting the data to Eq. (2) should reveal similar parameter values from both runs.

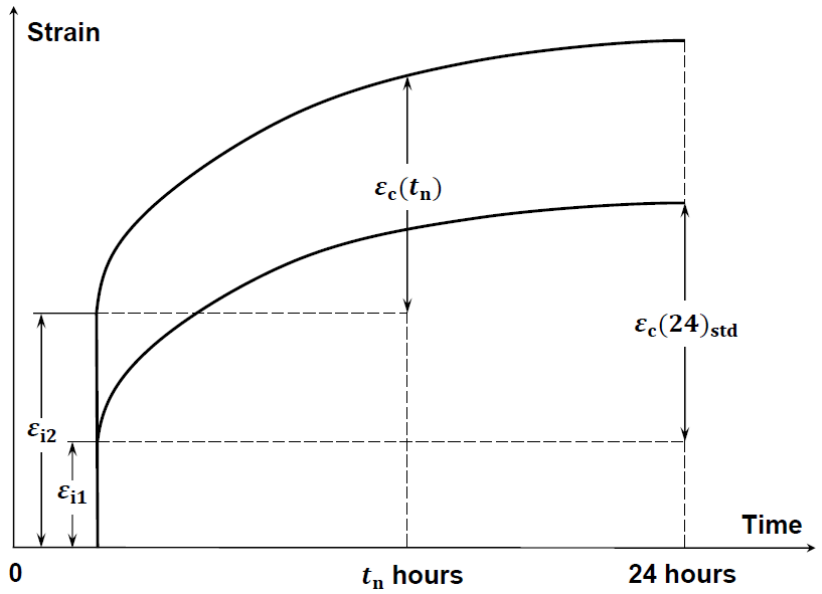

Fig. 2. Reducing the fibre creep time from 24 h to t_n by equalising the creep strain from a higher stress, $\varepsilon_c(t_n)$, with $\varepsilon_c(24)_{std}$.

The final step is to validate the effectiveness of VPPMCs produced under the t_n creep conditions. Since Charpy impact testing has been used for the majority of investigations into the performance of nylon fibre-based VPPMCs [1-6,8], this is the most appropriate evaluation method. Thus batches of VPPMC samples using t_n can be compared with similar batches produced under standard (24 h) creep conditions.

3. Experimental

3.1 Fibre evaluation

In contrast with previous VPPMC studies using nylon 6,6 fibre [1-6,8,9,11], the fibre used in this study was obtained from an industrial supplier, Ogden Fibres Ltd, UK. Both new and old (i.e. previously studied) fibre materials were continuous untwisted multifilament yarns of ~94 tex; however, scanning electron microscopy (SEM) was used to compare samples of new and old yarns, in terms of fibre topography, filament diameter and number of filaments per yarn.

To obtain long-term viscoelastic recovery and remove manufacturing-induced residual stresses, annealing of the yarn at 150°C for 0.5 h was an essential requirement [4,5]. Here, samples of yarn were placed, unconstrained, in a fan-assisted oven.

Following annealing, further examination of the new and old yarn samples was made by SEM.

3.2 Creep-recovery experiments

Experimental procedures for creep-recovery studies have been previously reported [2]. Briefly, a sample of yarn was annealed as described in Section 3.1. The yarn was then attached to a simple (force-calibrated) loading rig with counterbalanced platform to support weights for the creep cycle; however, at least 0.5 h was allowed to elapse between completing the annealing cycle and starting the creep cycle, for the yarn to regain its equilibrium moisture content. In situ evaluation of creep and (following load removal) recovery strain could be made by measuring the distance between two inked marks on the yarn (typically 300-400 mm apart). A digital cursor with a precision of ±0.01 mm was used for this purpose and all strain measurements were made under ambient conditions of 20.0-21.5°C and 30-40% RH.

Following initial trials, three 24 h creep loads were selected for detailed assessment, providing stress values of 330, 460 and 590 MPa. Here, 330 MPa represented a standard creep stress and the highest value (590 MPa) was found to be consistent with avoiding the risks of fibre damage outlined in Section 2. For repeatability, three samples of annealed yarn were subjected to creep at each of the three stress values and recovery strain was subsequently monitored after each 24 h creep run. By using Eq. (1) with these results, $\varepsilon_c(24)_{std}$ was determined from the 330 MPa creep data and data from 460 MPa and 590 MPa enabled the corresponding $\varepsilon_c(t_n)$ values to be obtained. Eq. (1) was fitted to the creep data using commercially available software (*CurveExpert 1.4*); this provided all the equation parameter values and the correlation coefficient to indicate quality of curve fitting. Although the standard applied stress was ~340 MPa in previous work (Section 2), the slightly lower stress of 330 MPa for $\varepsilon_c(24)_{std}$ resulted from minor changes in stretching rig calibration (using the same loading conditions) and the small difference in cross-sectional area between new and old yarns (Section 4.1).

Two further sets of three creep runs were performed, one at 460 MPa and the other at 590 MPa, over creep times equal to t_n in each case, to compare the recovery strain-time characteristics with those from the standard 24 h, 330 MPa creep data. Eq. (2) was used with the software for this purpose. Since the recovery characteristics might be expected to be similar, any significant deviation between the three data sets may indicate differences in viscoelastic creep-recovery mechanisms.

3.3 Production of composite samples

As with previous studies involving Charpy impact testing [1-6,8], open casting of composite samples in batches provided the simplest production method and mechanical evaluation required VPPMC ‘test’ samples to be compared with unstressed ‘control’ counterparts. To ensure no differences between test and control samples (other than prestress effects), each batch required the simultaneous production of test and control samples.

To produce one batch, two lengths of yarn (designated test and control) were simultaneously annealed as described in Section 3.1. The stretching rig (Section 3.2) was then used to subject the test yarn to the designated creep stress (330, 460 or 590 MPa) and duration (24 h for 330 MPa or t_n for 460 and 590 MPa), whilst the control

yarn was positioned (unconstrained) in close proximity for exposure to the same ambient conditions (20.0-21.5°C, 30-40% RH). On releasing the creep load, both yarns were cut to appropriate lengths and brushed into flat ribbons (for fibre separation) ready for moulding.

A clear-casting polyester resin was used for the matrix, i.e. Reichhold Polylite 32032, mixed with 2% MEKP catalyst, supplied by MB Fibreglass, UK. Room temperature gel-time was ~20 min. Unidirectional continuous fibre composite samples were produced by open casting from two aluminium moulds. Each mould had a 460 mm long, 10 mm wide channel, so that a strip of test and control materials could be cast simultaneously from the same resin mix. The process was completed within 0.5 h of the stretching operation and demoulding took place ~2 h after casting. The two composite strips were then each cut into five equal lengths, to produce a batch of five test and five control samples, the sample dimensions being 80 × 10 × 3.2 mm. All samples were held under a weighted steel strip for 24 h to prevent any sample distortion from residual stresses. Each batch of composite samples was then stored (in polyethylene bags) for 336 h (i.e. two weeks) prior to impact testing. A total of 15 batches were produced, all with a fibre volume fraction, V_f, of ~2.0%.

3.4 Charpy impact tests

Impact testing was achieved with a Ceast Resil 25 Charpy machine using a 7.5 J hammer at 3.8 ms^{-1}, operating in accordance with BS EN ISO 179. In previous work where low V_f open-cast polyester matrix composite samples have been studied, nylon 6,6 and polyethylene fibres [1-8,10] tended to settle towards the bottom of the mould before the resin cured. Therefore, impact testing was performed by mounting the samples with the fibre-rich side facing away from the pendulum hammer and a diagram showing this configuration has been previously published [1-3]. In accordance with earlier Charpy-based studies on low V_f nylon 6,6 fibre composite samples [1-5], a 24 mm span was adopted for this work.

4. Results and discussion

4.1 Fibre evaluation

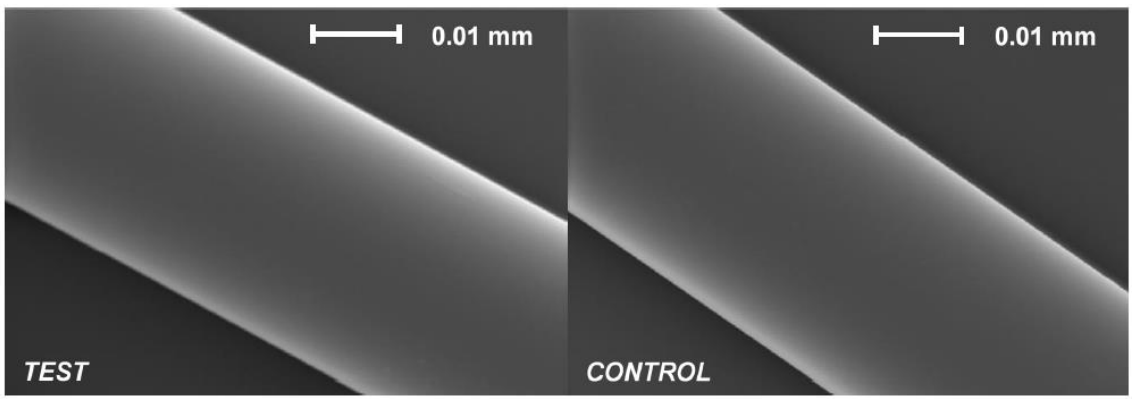

Fig. 3. SEM micrographs from the new yarn (annealed), showing test (24 h creep at 590 MPa) and control (no creep) fibre samples, 72 h after releasing the creep load for the test sample.

Examination of the new and old yarns in as-received and annealed forms by SEM revealed similar fibre topography. Following annealing, there were ~140 filaments of 26.0 ± 0.1 µm filament diameter in the new yarn, compared with ~135 filaments of 26.4 ± 0.1 µm filament diameter in the previously studied material. These small differences resulted in the cross-sectional area of the new yarn being marginally greater (<1%) than the old material, contributing to the slight reduction in applied stress for the standard creep run (Section 3.2). Fig. 3 shows samples of test and control fibres from the new yarn, the test fibres being previously subjected to 590 MPa creep stress for 24 h. There appear to be no differences in fibre topography, thus it may be inferred that there is no damage from the maximum (24 h) exposure to the highest stress value.

4.2 Fibre creep and recovery

Fig. 4(a) shows the creep strain-time data for the three loading values and the associated curve-fits using Eq. (1). The parameter values from Eq. (1) are listed in Table 1 and from Eq. (1), the $\varepsilon_c(24)_{std}$ value (330 MPa) was found to be 3.4%. Thus for $\varepsilon_c(t_n)$ equal to $\varepsilon_c(24)_{std}$, the t_n values from the 460 MPa and 590 MPa creep data were found to be 92 min and 37 min respectively.

The resulting recovery data from the 24 h creep runs in Fig. 4(a) are shown in Fig. 4(b) and the corresponding parameter values from Eq. (2) are also given in Table 1. Clearly, there is greater scatter within the recovery strain measurements in Fig. 4(b), compared with the creep strain data of Fig. 4(a) and this can be attributed to the yarns being held in a high state of tension for the latter case, which facilitated measurement. Nevertheless, the recovery parameters for 24 h creep at 330 MPa in Table 1 are comparable to those previously obtained with the old yarn material [4]. Of particular importance is that values for ε_f in Table 1, even from 24 h creep runs at the highest stress (590 MPa) are less than 10^{-4} %, i.e. (unwanted) viscous flow effects are predicted by Eq. (2) to be negligible.

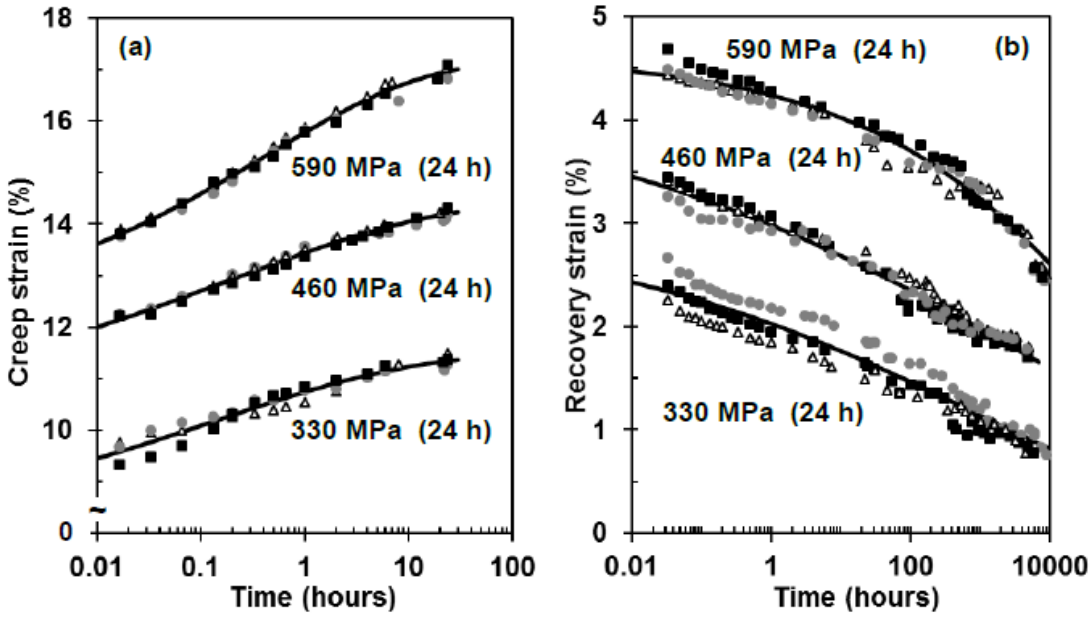

Fig. 4. Strain-time data for (a) 24 h creep and (b) recovery at the three stress values with curve-fits from Eq. (1) and Eq. (2).

Table 1. Summary of the creep and recovery parameters from data in Fig. 4 using Eq. (1) and Eq. (2); r is the correlation coefficient.

24 h applied stress (MPa)	Creep parameters					Recovery parameters				
	ε_c (%)	β_c	η_c (h)	ε_i (%)	r	ε_r (%)	β_r	η_r (h)	ε_f (%)	r
330	3.538	0.2245	0.1428	7.956	0.9729	3.052	0.1270	1155	$< 10^{-9}$	0.9651
460	4.317	0.2048	0.1889	10.181	0.9939	4.361	0.1056	9637	$< 10^{-4}$	0.9865
590	5.044	0.2830	0.4256	12.141	0.9957	4.621	0.2062	150468	$< 10^{-5}$	0.9853

Creep strain-time data at 460 MPa and 590 MPa for the corresponding t_n values (92 min and 37 min) are shown in Fig. 5, with the resulting recovery strain data. Again, it is encouraging to note that ε_f is less than 10^{-4} % in both cases. By comparing the recovery data from 330 MPa in Fig. 4(b) with the results in Fig. 5(b) and (d), it can be seen that higher creep stress values applied over shorter times increase the resulting recovery strain as a function of time.

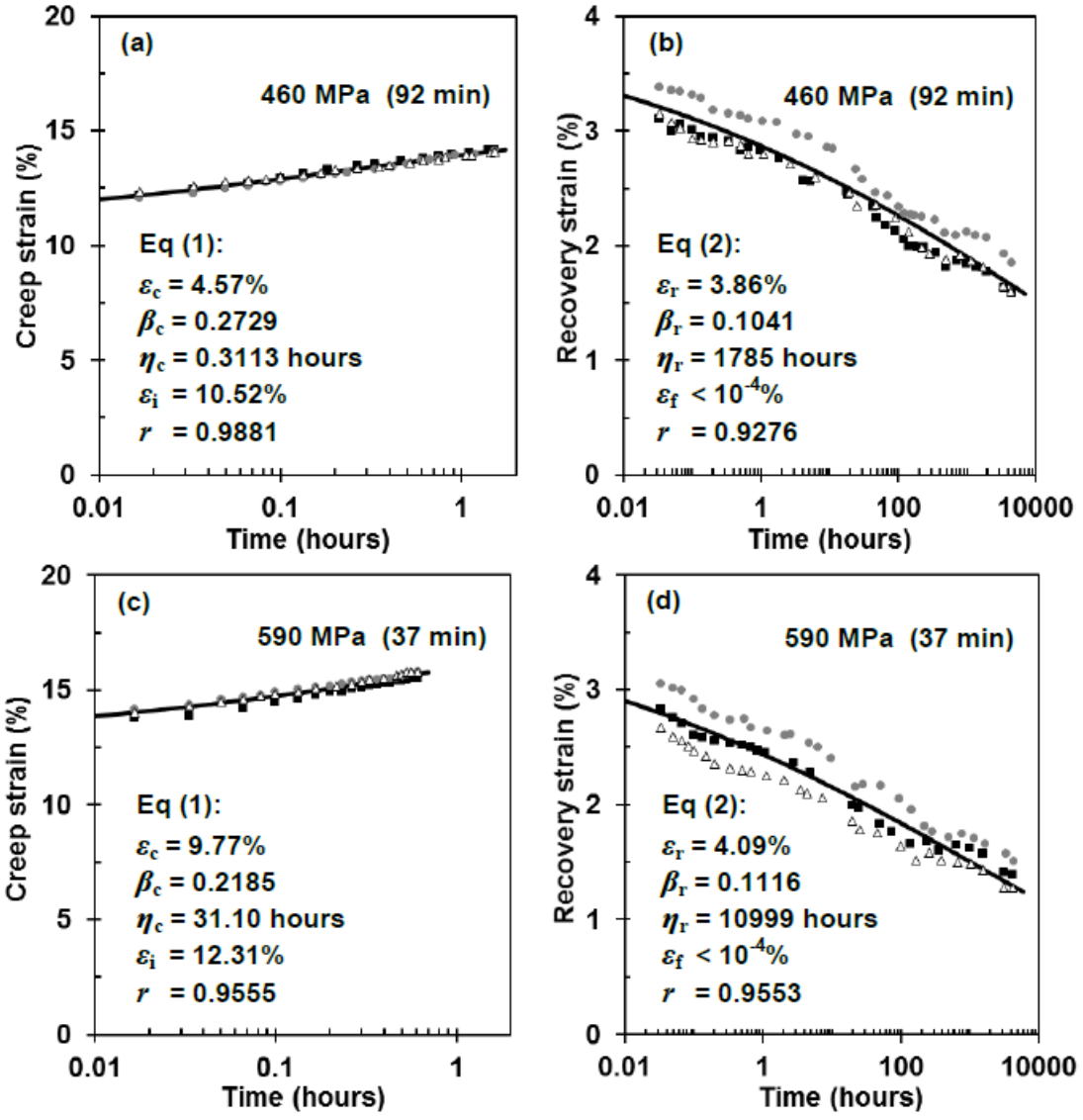

Fig. 5. Plots of creep strain to values of t_n for 460 MPa and 590 MPa, and the corresponding recovery strain-time data, with curve-fit parameters.

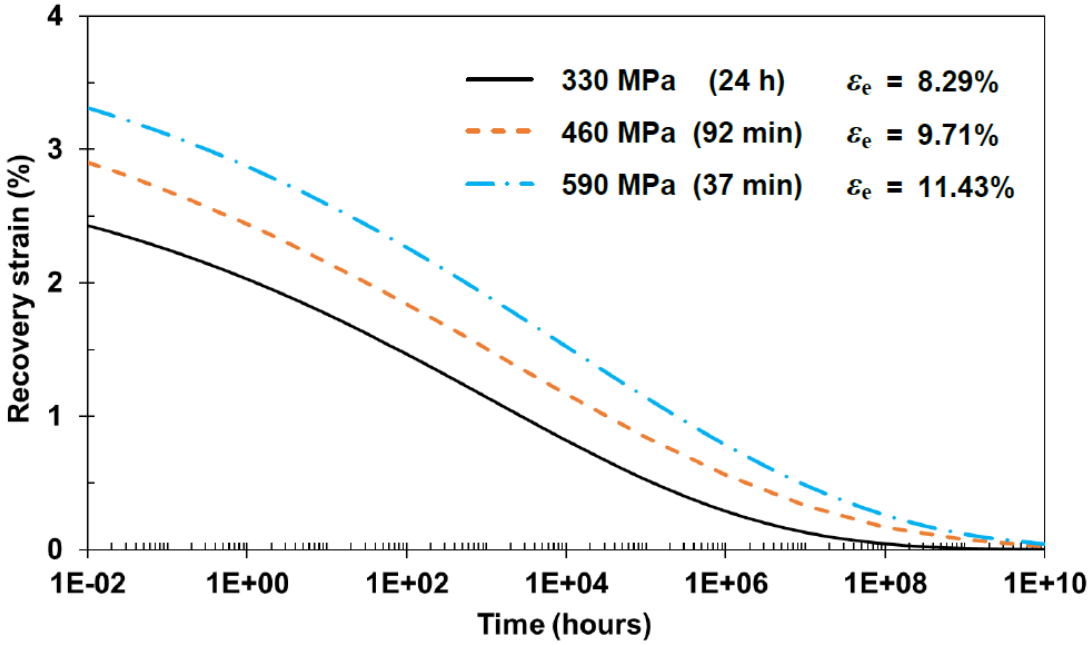

Fig. 6. Recovery curves from Figs. 4 and 5, using Eq. (2), plotted on common axes to show their offset. The ε_e result for each stress value was calculated by subtracting ε_i (Table 1 and Fig. 5) from the final creep strain value predicted by Eq. (1).

The effect is clarified by Fig. 6, which shows the curves from Eq. (2) plotted on common axes, over a much longer timescale. As suggested in Section 3.2, the recovery characteristics might be expected to be similar. Since the curves in Fig. 6 represent recovery data in which viscoelastic creep strain was equalised (Fig. 2), only the elastic strain components differed between the three creep stress levels. Although ε_i, the elastic strain at the onset of creep, increases with applied stress, the resulting elastic recovery strain, ε_e, should also increase and this is demonstrated by the calculated ε_e values in Fig. 6 corresponding with the ε_i data in Table 1 and Fig. 5 to within <1% strain.

The viscoelastic response during creep and recovery can be described by the action of sites triggered, through spring-dashpot time constants, by mechanical latches. On a molecular level, this can be envisaged as segments of molecules jumping between positions of relative stability [21,23]. Thus for a higher applied stress, more sites could be triggered earlier during creep, compared with creep applied at 330 MPa over the same timescale, and this enables t_n to be reduced accordingly to achieve the same level of viscoelastic creep strain. It is also possible that some of these sites are activated only at higher creep stress levels (i.e. >330 MPa) and, during recovery, their time-dependent triggering characteristics may differ in comparison with sites activated at 330 MPa. We suggest that this effect could provide an explanation for the offset between the three recovery curves in Fig. 6.

4.3 Charpy impact data

Data from the Charpy impact tests are summarised in Table 2 and Fig. 7. The results show little difference in impact energy absorption, either in relative or absolute terms. In fact, two-sided hypothesis testing has shown no difference between test sample means for the three prestressing conditions (5% significance level). The overall mean increase in impact energy, at ~56%, is higher than that from recent published

work (30–40%) with nylon 6,6 fibre VPPMCs [5,6] and this may be attributed to slight differences between the yarns (Section 4.1), polyester resin formulations and V_f.

Table 2. Charpy impact results. Five sample batches were tested for each prestressing condition (5 test and 5 control samples in each batch); SE is the standard error.

Batch	Mean impact energy (kJm^{-2})		Increase in energy (%)
	Test ± SE	Control ± SE	
330 MPa (24 h)	33.93 ± 3.14	23.78 ± 1.48	42.64
	37.02 ± 1.78	20.71 ± 0.63	78.76
	35.36 ± 1.71	25.03 ± 0.96	41.26
	36.71 ± 2.89	25.60 ± 1.15	43.37
	35.58 ± 1.96	21.61 ± 1.13	64.69
Mean ± SE	35.72 ± 0.99	23.35 ± 0.59	54.14 ± 7.52
460 MPa (92 min)	40.35 ± 2.81	25.93 ± 1.16	55.59
	39.42 ± 1.95	24.58 ± 1.05	60.35
	37.82 ± 1.86	23.24 ± 1.13	62.78
	33.87 ± 1.21	21.97 ± 0.85	54.20
	37.37 ± 1.67	22.83 ± 0.42	63.66
Mean ± SE	37.77 ± 0.92	23.71 ± 0.48	59.32 ± 1.90
590 MPa (37 min)	34.43 ± 3.68	24.62 ± 1.12	39.86
	38.59 ± 2.24	23.31 ± 0.79	65.58
	37.17 ± 4.06	25.00 ± 0.98	48.68
	37.51 ± 1.32	23.56 ± 0.94	59.21
	37.97 ± 2.77	24.27 ± 0.72	56.44
Mean ± SE	37.14 ± 1.25	24.15 ± 0.40	53.95 ± 4.45

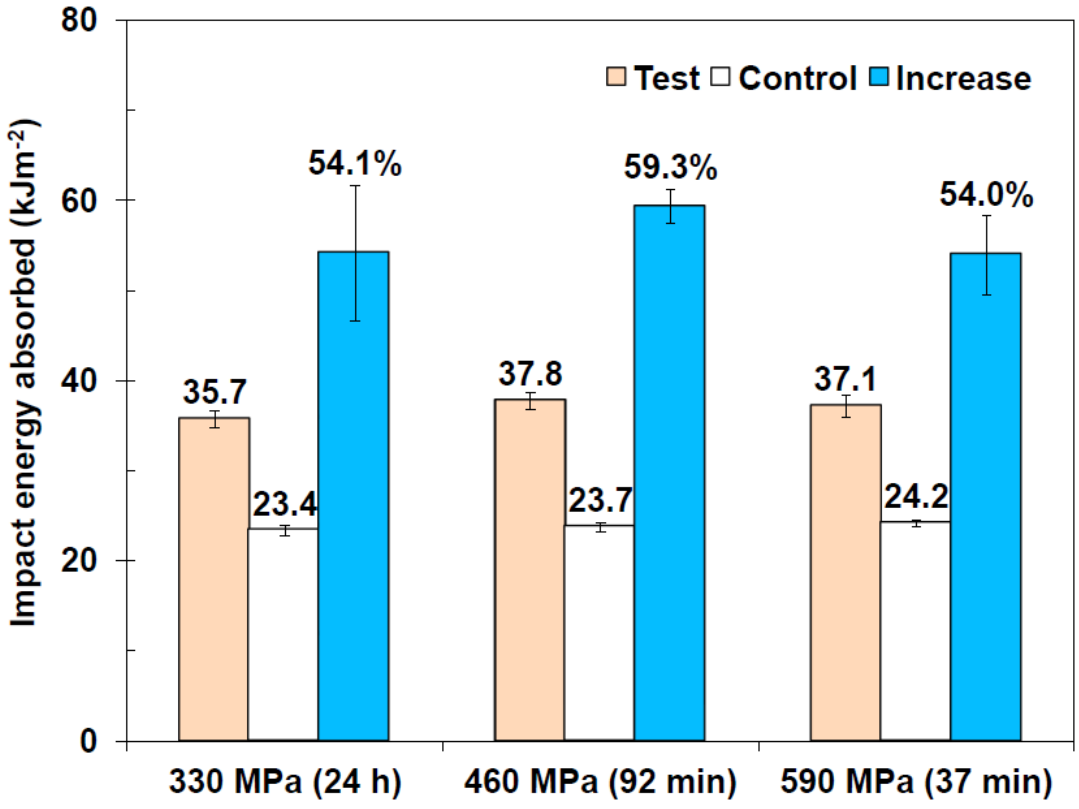

Fig. 7. Charpy impact test results from Table 2; error bars represent the standard error.

Fig. 8 shows typical test and control samples following impact testing. In correspondence with the data, there appear to be no discernible differences in the fracture characteristics between the three conditions. The greater area of fibre-matrix debonding observed in the test samples is consistent with findings from previous studies of VPPMCs based on nylon 6,6 fibre [1-6]. Although all four mechanisms for mechanical property improvements cited in Section 1 may contribute towards increased impact energy absorption in the test samples, mechanism (iv) is the main factor [6]. This mechanism, i.e. residual shear stresses at the fibre–matrix interface regions promoting (energy absorbing) debonding over transverse fracture, explains the larger area of debonding (hence increased energy absorption) seen in the test samples in Fig. 8.

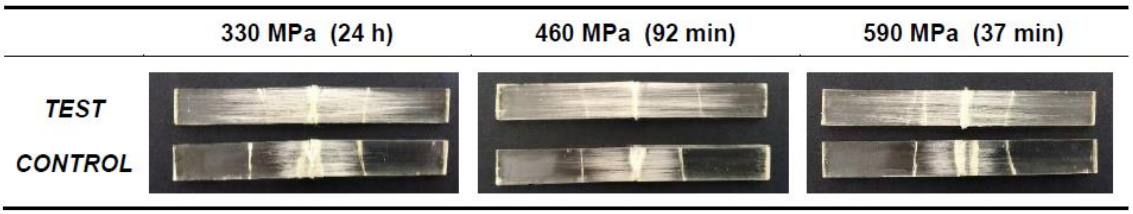

Fig. 8. Representative test and control samples following Charpy impact testing, showing similar debonding and fracture characteristics from the three creep conditions; note the larger area of fibre-matrix debonding in the test samples.

Since all impact tests were performed on samples at 336 h, the results can be compared with viscoelastic recovery strain data at the same age. From Fig. 6, the recovery strains at 336 h are approximately 1.3%, 1.7% and 2.1% from creep at the 330 MPa, 460 MPa and 590 MPa runs respectively and these differences may be attributed to possible changes in triggering sites (Section 4.2). Nevertheless, when these recovery strains are subtracted from their respective ε_r (at $t = 0$) values in Table 1 and Fig. 5, the resulting elapsed viscoelastic recovery strains (at 336 h) are approximately 1.8% (330 MPa), 2.2% (460 MPa) and 2.0% (590 MPa); i.e. they are similar. Since these strain values can be expected to relate directly to prestress levels in the VPPMC samples at 336 h, there is concurrence with the Charpy impact test data. Previous studies into the force output–time characteristics of viscoelastically recovering fibres [7,10,24] have provided useful insights into fibre behaviour and future work with this technique should facilitate a further understanding of the findings from this study.

4.4 Towards process optimisation: further considerations

As a consequence of the findings from this work, the possibility of a general relationship between applied creep stress and t_n can be considered, as shown in Fig. 9. Although only three data points are available, Fig. 9 indicates a simple logarithmic trend, thus it may be possible to predict the required stress for a designated t_n value. Clearly, more experimental runs would be required for the plot in Fig. 9 to provide reliable predictions; however, the current line-fit suggests that an increase in applied stress to, for example, 1 GPa could reduce t_n to within 6 min.

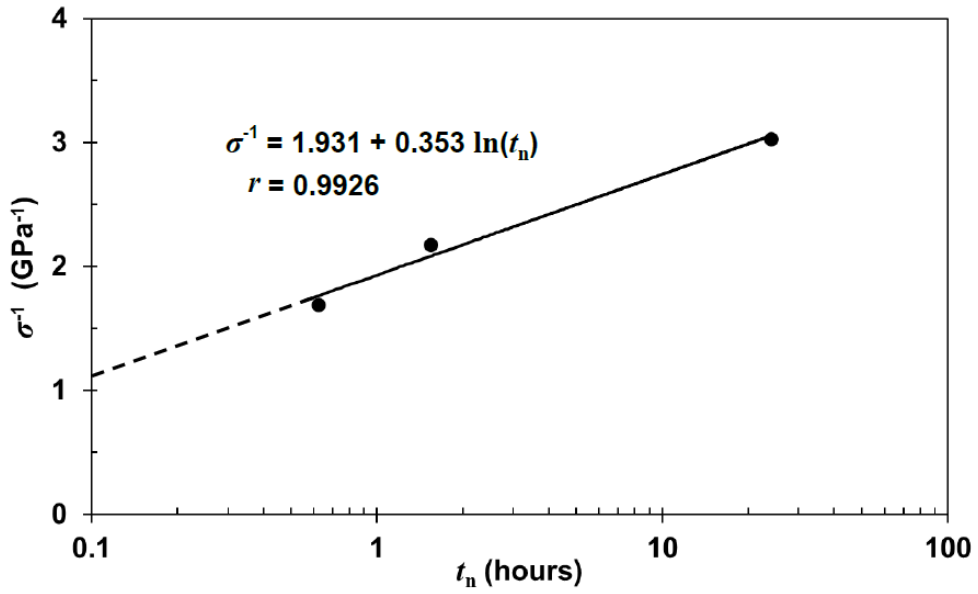

Fig. 9. Plot showing relationship between applied creep stress σ and t_n.

Although the current work has demonstrated that VPPMC performance from fibres subjected to 37 minutes of creep at 590 MPa is equivalent to 24 h at 330 MPa, it is clear from Fig. 4 that these fibres can sustain 24 h at 590 MPa without creep-induced fracture. Thus a longer exposure to 590 MPa may provide increased prestress generation, thereby offering possibilities for further improvements to VPPMC performance. This aspect will be investigated in a future study.

5. Conclusions

This study has taken the first steps towards process optimisation by investigating the feasibility of reducing the creep loading period for VPPMC production. By using nylon 6,6 fibres, our main findings are:

(i) The previously adopted viscoelastic creep strain, which requires a tensile stress of 330 MPa for 24 h, can be achieved over a shorter duration, t_n, using increased creep stress. Thus t_n was 92 min at 460 MPa and 37 min at 590 MPa. Subject to avoiding fibre damage however, it may be possible to reduce t_n further.

(ii) Although there was some offset between viscoelastic recovery strain–time curves from the three creep settings, elapsed recovery strain values were similar. The latter concurred with Charpy impact test data from VPPMC samples corresponding to the three creep settings, as there were no significant differences in impact energy absorption, these being ~56% greater than their control (unstressed) counterparts.

Future work will focus on producing a generalised relationship between t_n, creep stress and fibre viscoelastic recovery characteristics (strain and force output).

Acknowledgements

Support from the Hull-China Scholarship Council scheme for one of the authors (BW) is gratefully acknowledged. The authors also wish to thank Garry Robinson from the School of Engineering for technical support.

References

[1] Fancey KS. Investigation into the feasibility of viscoelastically generated pre-stress in polymeric matrix composites. Mater Sci Eng A 2000; 279(1-2):36-41.
[2] Fancey KS. Prestressed polymeric composites produced by viscoelastically strained nylon 6,6 fibre reinforcement. J Reinf Plast Compos 2000; 19(15):1251-1266.
[3] Fancey KS. Fibre-reinforced polymeric composites with viscoelastically induced prestress. J Adv Mater 2005; 37(2):21-29.
[4] Pang JWC, Fancey KS. An investigation into the long-term viscoelastic recovery of Nylon 6,6 fibres through accelerated ageing. Mater Sci Eng A 2006; 431(1-2):100-105.
[5] Fancey KS. Viscoelastically prestressed polymeric matrix composites – Potential for useful life and impact protection. Compos Part B 2010; 41(6):454-461.
[6] Fazal A, Fancey KS. Viscoelastically prestressed polymeric matrix composites – Effects of test span and fibre volume fraction on Charpy impact characteristics. Compos Part B 2013; 44(1):472-479.
[7] Fazal A, Fancey KS. UHMWPE fibre-based composites: Prestress-induced enhancement of impact properties. Compos Part B 2014; 66:1-6.
[8] Fazal A, Fancey KS. Performance enhancement of nylon/Kevlar fiber composites through viscoelastically generated pre-stress. Polym Compos 2014; 35:931-938.
[9] Pang JWC, Fancey KS. The flexural stiffness characteristics of viscoelastically prestressed polymeric matrix composites. Compos Part A 2009; 40(6-7):784-790.
[10] Fazal A, Fancey KS. Viscoelastically generated prestress from ultra-high molecular weight polyethylene fibres. J Mater Sci 2013; 48:5559-5570.
[11] Pang JWC, Fancey KS. Analysis of the tensile behaviour of viscoelastically prestressed polymeric matrix composites. Compos Sci Tech 2008; 68(7-8):1903-1910.
[12] Zhigun IG. Experimental evaluation of the effect of prestressing the fibers in two directions on certain elastic characteristic of woven-glass reinforced plastics. Mech Compos Mater 1968; 4(4-6):691-695.
[13] Tuttle M.E. A Mechanical/Thermal Analysis of Prestressed Composite Laminates. J Compos Mater 1988; 22(8):780-792.
[14] Tuttle ME, Koehler RT, Keren D. Controlling thermal stresses in composites by means of fiber prestress. J Compos Mater 1996; 30(4):486-502.
[15] Hadi AS, Ashton JN. On the influence of pre-stress on the mechanical properties of a unidirectional GRE composite. Compos Struct 1998; 40(3-4):305-311.
[16] Motahhari S, Cameron J. Impact strength of fiber pre-stressed composites. J Reinf Plast Compos 1998; 17(2):123-130.
[17] Motahhari S, Cameron J. Fibre prestressed composites: improvement of flexural properties through fibre prestressing. J Reinf Plast Compos 1999; 18(3):279-288.

[18] Schlichting LH, de Andrada MAC, Vieira LCC, Barra GMD, Magne P. Composite resin reinforced with pre-tensioned glass fibers. Influence of prestressing on flexural properties. Dent Mater 2010; 26(2):118-125.
[19] Nishi Y, Okada T, Okada S, Hirano M, Matsuda M, Matsuo A, Faudree MC. Effects of tensile prestress level on impact value of 50 vol% continuous unidirectional 0 degree oriented carbon fiber reinforced epoxy polymer (CFRP). Mater Trans 2014; 55:318-322.
[20] Cui H, Guan M, Zhu Y, Zhang Z. The flexural characteristics of prestressed bamboo slivers reinforced parallel strand lumber (PSL). Key Eng Mater 2012; 517:96-100.
[21] Fancey KS. A latch-based Weibull model for polymeric creep and recovery. J. Polym. Eng 2001; 21(6):489-509.
[22] Howard WH, Williams ML. The viscoelastic properties of oriented nylon 66 fibers: part I: creep at low loads and anhydrous conditions. Textile Res J 1963; 33(9):689-696.
[23] Fancey KS. A mechanical model for creep, recovery and stress relaxation in polymeric materials. J Mater Sci 2005; 40(18):4827-4831.
[24] Pang JWC, Lamin BM, Fancey KS. Force measurement from viscoelastically recovering Nylon 6,6 fibres. Mat Lett 2008; 62(10-11):1693-1696.